

# Proteomic analysis of the monkey hippocampus for elucidating ischemic resistance

Yurie Mori,<sup>1</sup> Shinji Oikawa,<sup>1,\*</sup> Shota Kurimoto,<sup>1</sup> Yuki Kitamura,<sup>1,2</sup> Saeko Tada-Oikawa,<sup>1,3</sup> Hatasu Kobayashi,<sup>1</sup> Tetsumori Yamashima,<sup>4</sup> and Mariko Murata<sup>1</sup>

<sup>1</sup>Department of Environmental and Molecular Medicine, Mie University Graduate School of Medicine, Edobashi 2-174, Tsu, Mie 514-8507, Japan

<sup>2</sup>College of Pharmacy, Kinjo Gakuin University, 2-1723 Omori, Moriyama-ku, Nagoya, Aichi 463-8521, Japan

<sup>3</sup>Department of Human Nutrition, School of Life Studies, Sugiyama Jogakuen University, 17-3 Hoshigaoka-motomachi, Chikusa-ku, Nagoya, Aichi 464-8662, Japan

<sup>4</sup>Departments of Psychiatry and Neurobiology, Kanazawa University Graduate School of Medical Science, Takakura-machi 13-1, Kanazawa, Ishikawa 920-8641, Japan

(Received 26 August, 2019; Accepted 13 January, 2020; Published online 9 April, 2020)

It is well-known that the cornu *Ammonis* 1 (CA1) sector of hippocampus is vulnerable for the ischemic insult, whereas the dentate gyrus (DG) is resistant. Here, to elucidate its underlying mechanism, alternations of protein oxidation and expression of DG in the monkey hippocampus after ischemia-reperfusion by the proteomic analysis were studied by comparing CA1 data. Oxidative damage to proteins such as protein carbonylation interrupt the protein function. Carbonyl modification of molecular chaperone, heat shock 70 kDa protein 1 (Hsp70.1) was increased remarkably in CA1, but slightly in DG. In addition, expression levels of nicotinamide adenine dinucleotide (NAD)-dependent protein deacetylase sirtuin-2 (SIRT2) was significantly increased in DG after ischemia, but decreased in CA1. Accordingly, it is likely that SIRT2 upregulation and negligible changes of carbonylation of Hsp70.1 exert its neuroprotective effect in DG. On the contrary, carbonylation level of dihydropyrimidinase related protein 2 (DRP-2) and L-lactate dehydrogenase B chain (LDHB) were slightly increased in CA1 as shown previously, but remarkably increased in DG after ischemia. It is considered that DRP-2 and LDHB are specific targets of oxidative stress by ischemia insult and high carbonylation levels of DRP-2 may play an important role in modulating ischemic neuronal death.

**Key Words:** hippocampus, dentate gyrus, oxidative stress, proteomics, carbonylation

Oxidative damage due to ischemia-reperfusion has been implicated as one of the leading causes for cell death in a number of diseases such as cardiovascular diseases and neurological disorders.<sup>(1–4)</sup> The brain is particularly vulnerable to oxidative stress, because it consumes large amounts of oxygen compared to other organs.<sup>(5)</sup> Oxidative stress refers to a cell's state characterized by excessive production of reactive oxygen species (ROS). ROS, such as hydroxyl radicals ( $\cdot\text{OH}$ ), participate in damaging the cytoplasmic proteins, membrane lipids and DNA.<sup>(6,7)</sup> Oxidative damage to proteins can disrupt active site of enzymes, affect the conformation of structural proteins, and interrupt the protein function.<sup>(8,9)</sup> Protein carbonylation, the major and most common oxidative modification of proteins,<sup>(10)</sup> has been extensively focused to monitor oxidative damage due to its irreversible and irreparable nature,<sup>(11)</sup> and shown to affect the function and/or metabolic stability of the modified proteins.<sup>(12)</sup> Thus, protein carbonyls are likely to play an important role in the pathophysiology of disorders associated with oxidative stress.

Previous studies demonstrated that hippocampus, crucial for learning and memory processes, is extremely vulnerable to oxidative stresses.<sup>(13–19)</sup> Especially, the cornu *Ammonis* 1 (CA1) sector of

hippocampus is known to be extremely vulnerable to the ischemic insult than the dentate gyrus (DG).<sup>(20)</sup> Our previous study demonstrated carbonyl modification of heat shock 70 kDa protein 1 (Hsp70.1) in CA1 after the ischemia-reperfusion, and suggested that oxidative damage of Hsp70.1 may cause autophagy/lysosomal failure, leading to neuronal death.<sup>(21)</sup>

In this study, to clarify the mechanism of resistance to oxidative stress in DG, we investigated alternations of protein carbonylation and expression levels in DG of Japanese monkeys (*Macaca fuscata*) after the transient whole brain ischemia. The identification and characterization of carbonyl-modified proteins in the postischemic monkey DG were done by two-dimensional gel electrophoresis (2DE) with immunochemical detection of protein carbonyls (2D Oxyblot) and peptide mass fingerprinting (PMF). We also examined alternations of protein expression in DG after the ischemia-reperfusion, using two-dimensional differential in-gel electrophoretic analysis (2D DIGE). In addition, to elucidate the difference of vulnerability against oxidative stress between DG and CA1, we compared alteration of carbonyl levels in DG after the ischemia-reperfusion with those in CA1, which we previously reported.<sup>(21)</sup>

## Materials and Methods

**Sample preparation.** All experimental procedures were performed in adherence with the guidelines of the Animal Care and Ethics Committee of Kanazawa University (Approval No.: AP-132874) and the NIH Guide for the Care and Use of Laboratory Animals. The monkeys used in this study were 12 adult (5–11 years of age) Japanese monkeys (*Macaca fuscata*) with body weight of 5–10 kg. We operated ischemia-reperfusion according to the procedure previously described.<sup>(22,23)</sup> Briefly, after removal of the sternum, the innominate and left subclavian arteries were exposed in the mediastinum and were clipped for 20 min, then reperfusion was done. The effectiveness of clipping was demonstrated by an almost complete absence of cerebral blood flow, which was monitored by laser Doppler (Vasamedics, St. Paul, MN). Hippocampal DG and CA1 tissues were resected from both the sham-operated controls ( $n = 3$ ), postischemic day 3 ( $n = 3$ ), day 5 ( $n = 3$ ) and day 7 ( $n = 3$ ) monkeys at indicated time points after the ischemic insult under the general anaesthesia.<sup>(23)</sup> The control monkeys were dissected on the same day of sham operation. Dissected fresh samples were immediately put into the liquid nitrogen and stored at  $-80^{\circ}\text{C}$  until use.

\*To whom correspondence should be addressed.  
E-mail: s-oikawa@doc.medic.mie-u.ac.jp

Frozen tissue (20–30 mg) was directly transferred into a reaction tube containing 100  $\mu$ l of lysis buffer (30 mM Tris-HCl, 7 M urea, 2 M thiourea, 4% w/v 3-[(3-cholamidopropyl) dimethylammonio] propanesulfonate (CHAPS), a protease inhibitor cocktail, pH 8.5). The tissue samples were homogenized using the Sample Grinding Kit (GE Healthcare UK Ltd., Buckinghamshire, England) and incubated for 60 min on ice. All samples were centrifuged at  $30,000 \times g$  for 30 min at 4°C. The supernatant was collected and stored at –80°C. Total protein of sample was quantified by the Bradford assay, using bovine serum albumin as standard.<sup>(24)</sup>

**Detection of carbonyl modified proteins (2D Oxyblot analysis).** The mixed protein samples (100  $\mu$ g protein) were prepared by combining equal amounts (33  $\mu$ g) of three different samples from each group (control, days 3, 5 and 7). Carbonylated proteins in the mixed protein samples (100  $\mu$ g protein) were labeled by derivatization of carbonyl group with 2,4-dinitrophenylhydrazine (DNPH) by reaction with 2,4-dinitrophenylhydrazine (DNPH) and separated by 2DE. Proteins were transferred onto the PVDF membranes (Immobilon-P Transfer Membrane, Millipore, Darmstadt, Germany), using TE77 semi-dry transfer unit (GE Healthcare, Buckinghamshire, England). Transferred membranes were blocked and incubated with anti-DNPH rabbit polyclonal antibody.<sup>(21)</sup> The chemiluminescence signal was detected on X-ray films. The spot intensities of carbonylated proteins were quantified using PDQuest ver. 8.0 (Bio-Rad, California, CA). We repeatedly confirmed reproducibility of 2D Oxyblot analysis. The specific oxidation was estimated as relative carbonyl level (obtained from 2D Oxyblot) per relative protein expression (obtained from 2D DIGE). For the protein identification, spots were excised from 2D gels obtained with non-DNPH-treated samples and analyzed by the mass spectrometry.

**Two-dimensional differential in-gel electrophoretic (2D DIGE) analysis.** Samples were labeled using CyDyes DIGE Fluor (minimal dye) labeling kit (GE Healthcare). Samples (25  $\mu$ g protein) were labeled with minimal fluorescent dye and incubated on ice for 30 min in the dark. Then, each Cy3 labeled samples were combined with an equal amount of Cy5 labeled samples, and

the pooled Cy2 labeled sample was added as an internal standard and mixed each batch. First dimension, isoelectric focusing (IEF), was performed on IPG strips (IPG, pH 3–10 NL strips, 24 cm, GE Healthcare) and an Ettan IPGphor isoelectric focusing system (GE Healthcare). Samples labeled with fluorescent dye were applied strips on the reswelling tray and focused. After focusing, proteins were separated by 2DE.<sup>(21)</sup> The 2D DIGE gels were scanned in a Typhoon FLA 9500 (GE Healthcare). Spot detection, gel matching, and statistical analysis were performed with DeCyder 2D software ver. 7.2 (GE Healthcare). Protein expression values were statistically analyzed using Student's *t* test.

**Protein identification.** The method used was essentially as described by Kondo *et al.*<sup>(25)</sup> with some modifications. Preparative 2DE gels were visualized by CBB-stained. The protein spots picking were performed manually, were destained four times, dehydrated twice, and digested with trypsin (Promega, Madison, WI) solution for overnight at 37°C. The peptide solutions were eluted with 45% acetonitrile/0.1% trifluoroacetic acid (TFA) and concentrated. The peptide solutions containing 50%  $\alpha$ -cyano-4-hydroxycinnamic acid (Wako Pure Chemical, Osaka, Japan) were spotted on a MALDI plate. Mass analysis was performed with a matrix-assisted laser desorption ionization time-of-flight tandem mass spectrometry (MALDI-TOF/TOF MS; 4800 *Plus* MALDI-TOF/TOF<sup>TM</sup> Analyzer, AB SCIEX, Framingham, MA). Protein identification was performed with the MS/MS ion search tool in ProteinPilot software (AB SCIEX).

## Results

**Carbonylated proteins in DG after the ischemia-reperfusion.** To determine protein oxidation levels, protein carbonyls were studied by the 2D Oxyblot analysis of DNPH-treated samples, using an anti-DNP antibody. Figure 1 shows carbonylated proteins in the representative 2D Oxyblots from the DG of the control and day 5 after ischemia. A total of 192 carbonylated protein spots were detected in the DG. Among them, we focused on 4 spots which showed more than 5-fold increases in carbonylation at both

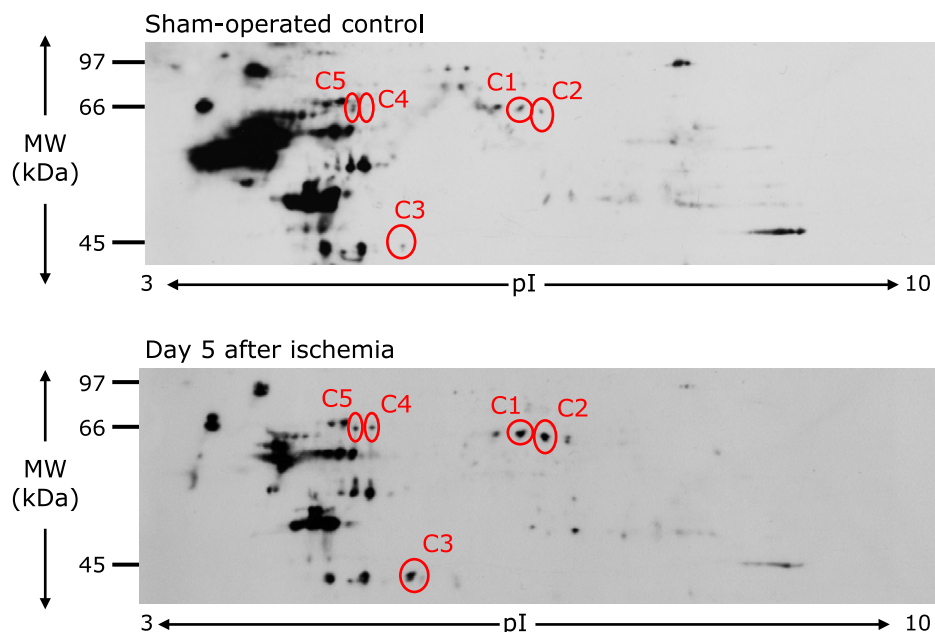


**Fig. 1.** 2D Oxyblot analysis of DG of the sham-operated control (top) and day 5 (bottom) after the ischemia-reperfusion insult. Proteins (100  $\mu$ g) were treated with DNPH and separated by 2DE, and transferred onto a PVDF membrane. Membrane was incubated with anti-DNP primary antibody, followed by incubation with horseradish peroxidase-conjugated secondary antibody. The reaction was visualized with ECL. The images obtained were processed using PDQuest ver. 8.0 (Bio-Rad Laboratories Ltd.) to match spots and provide spot volumes. The spots were identified by PMF.

**Table 1.** Identification of carbonylated protein based on PMF

| Spot number <sup>a)</sup> | % Cov <sup>b)</sup> | Protein name <sup>c)</sup>                    | MW <sup>d)</sup> | pI <sup>e)</sup> | Functional role  |
|---------------------------|---------------------|---|------------------|------------------|------------------|
| C1                        | 28.3                | Dihydropyrimidinase related protein 2 (DRP-2) | 73,583           | 5.94             | Axonal growth    |
| C2                        | 26.2                |   |                  |                  |                  |
| C3                        | 26.7                | L-lactate dehydrogenase B chain (LDHB)        | 36,927           | 5.85             | Metabolic enzyme |

<sup>a)</sup>Spot number as indicated in Fig. 1. <sup>b)</sup>Coverage of the matched peptides in relation to the full-length sequence. <sup>c)</sup>Proteins identified by 2D-gel fingerprinting. <sup>d)</sup>Theoretical molecular weight and <sup>e)</sup>theoretical isoelectric point were searched using the ExPASy Compute pI/Mw tool in ExPASy website (<http://www.expasy.org>).

days 3 and 5 after ischemia, compared to control. Among the 5 selected proteins, 3 spots could be identified by the mass spectrometry analysis followed by database matching. The spots of up-regulated carbonylated proteins were identified as dihydropyrimidinase related protein 2 (spot No. C1, C2) and L-lactate dehydrogenase B chain (spot No. C3). Information of these spots was described in Table 1, including the percentage of sequence coverage, protein name, theoretical molecular weight, theoretical pI-value, and functional role. The specific oxidation of each spot was calculated as relative carbonyl level per relative protein expression obtained from 2D DIGE. Figure 2 shows time course of the changes in the specific oxidation level.

#### Protein expression profiles in DG after ischemia-reperfusion.

We used 2D DIGE to investigate the protein expression profiles in DG at days 3, 5 and 7 after ischemia. Figure 3 shows the 2D DIGE image of DG lysates from the control and day 5 after ischemia. We detected spots on the 6 gels as determined by DeCyder Differential Analysis Software. A total of 2,372 protein spots were detected. Sixty-nine protein spots were significantly altered in the DG tissues of day 7 after ischemia, compared to the sham-operated control ( $p$  value  $<0.05$  and relative protein expression level  $>|1.10|$ ,  $n = 3$ /each group). Spots that were not detected in the Coomassie brilliant blue post-stained gel or poor quality spots were omitted. Finally, 8 differentially expressed spots could be identified by MALDI-TOF/TOF peptide mass fingerprinting (Table 2). The positions of the 8 spots (white circle) on the 2D gel are shown in Fig. 3.

The spots of up-regulated proteins were identified as NAD-dependent protein deacetylase sirtuin-2 (spot No. 1230), inorganic pyrophosphatase (spot No. 1396) and heat shock protein  $\beta$ -1 (spot No. 1739). The spots of down-regulated protein were identified

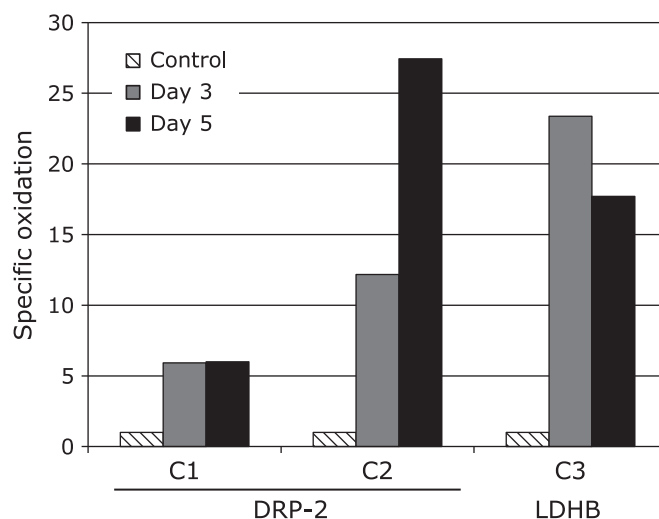


**Fig. 2.** The time course of specific oxidation levels. Spot numbers are shown in Table 1 and Fig. 1. Data were presented by fold changes in the ischemia-reperfusion brains, being compared with the controls. The specific oxidation of each spot was calculated as relative carbonyl level per relative protein expression obtained from 2D DIGE.

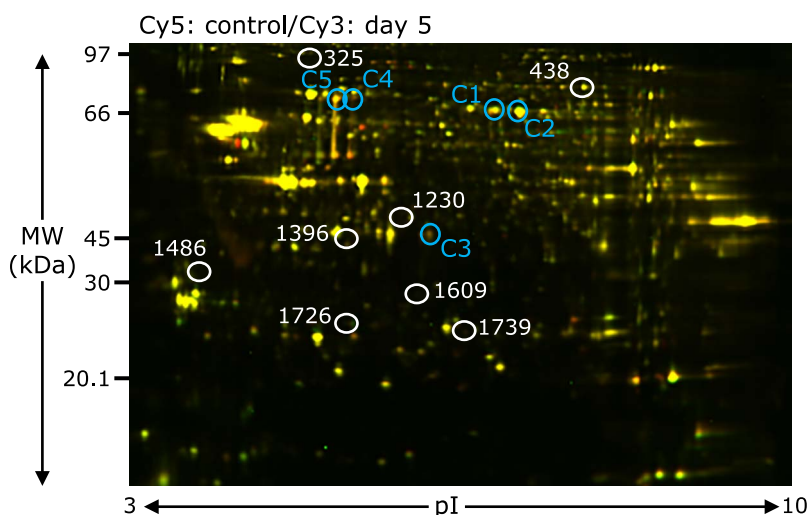


**Fig. 3.** 2D DIGE analyses of the control and day 5 postischemic DG. Proteins (25  $\mu$ g) were labeled with Cy3 (red) or Cy5 (green) dyes, mixed and subjected to 2D DIGE analysis. Red spots indicate upregulated proteins on day 5 after the ischemic insult, while green spots indicate downregulated proteins. Yellow spots represent proteins that were unchanged. 8 differentially expressed spots (white circle) could be identified. The blue circle spots correspond to C1–C5 in Fig. 1. See color figure in the on-line version.

**Table 2.** Identification of differentially expressed protein spots in DG

| Spot number <sup>a)</sup> | Protein name                                | % Cov <sup>b)</sup> | pI <sup>c)</sup> | MW <sup>d)</sup> | Relative protein expression level |       |       |       |
|---------------------------|---|---------------------|------------------|------------------|-----------------------------------|-------|-------|-------|
|                           |   |                     |                  |                  | Cont                              | Day 3 | Day 5 | Day 7 |
| 325                       | Heat shock cognate 71 kDa protein           | 13.2                | 5.37             | 70,898           | 1                                 | 0.92  | 0.88  | 0.79* |
| 438                       | Vesicle-fusing ATPase                       | 12.5                | 6.52             | 82,626           | 1                                 | 1     | 1     | 0.84* |
| 1230                      | NAD-dependent protein deacetylase sirtuin-2 | 12.3                | 5.22             | 43,182           | 1                                 | 1.25* | 1.23* | 1.44* |
| 1396                      | Inorganic pyrophosphatase                   | 31.5                | 5.66             | 32,743           | 1                                 | 1.03  | 1.08  | 1.20* |
| 1486                      | Tropomyosin $\alpha$ -3 chain               | 25.4                | 4.75             | 29,007           | 1                                 | 0.96  | 0.91  | 0.90* |
| 1609                      | Enoyl-CoA delta isomerase 1, mitochondrial  | 9.3                 | 8.80             | 32,816           | 1                                 | 0.96  | 0.88* | 0.88* |
| 1726                      | PITH domain-containing protein 1            | 24.2                | 5.47             | 24,178           | 1                                 | 0.91  | 0.88  | 0.79* |
| 1739                      | Heat shock protein $\beta$ -1               | 21.0                | 5.98             | 22,783           | 1                                 | 1.31  | 1.27* | 1.27* |

<sup>a)</sup>Spot number as indicated in Fig. 3. <sup>b)</sup>Coverage of the matched peptides in relation to the full-length sequence. <sup>c)</sup>Theoretical isoelectric point and <sup>d)</sup>theoretical molecular weight were searched using the ExPASy Compute pI/Mw tool in ExPASy website (<http://www.expasy.org>). \* $p < 0.05$  compared to the control.

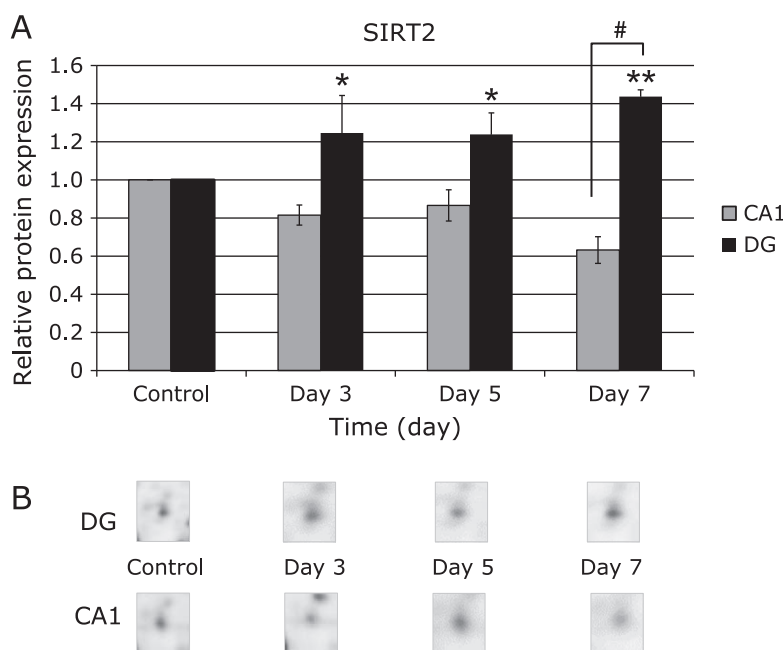


**Fig. 4.** The time course of SIRT2 expression in DG and CA1 after the ischemia-reperfusion. (A) Graphical expression profile of SIRT2 spot. Data was presented by fold changes after the ischemia-reperfusion, being compared with the control; \* $p < 0.05$ , \*\* $p < 0.01$  vs non-ischemic controls. # indicates a significant difference between DG and CA1 at 7 days after the ischemia-reperfusion by  $t$  test ( $p < 0.01$ ). (B) The representative SIRT2 spot image of 2D DIGE analysis.

as tropomyosin  $\alpha$ -3 chain (spot No. 1486), heat shock cognate 71 kDa protein (spot No. 325), vesicle-fusing ATPase (spot No. 438), enoyl-CoA delta isomerase 1, mitochondrial (spot No. 1609) and PITH domain-containing protein 1 (spot No. 1726).

Figure 4 shows the time course of the protein expression profiles of nicotinamide adenine dinucleotide (NAD)-dependent protein deacetylase sirtuin-2 (SIRT2) by comparing DG and CA1. SIRT2 was significantly increased in the DG at days 3, 5 and 7 after ischemia, but was decreased in the CA1.

## Discussion

### Alternations of carbonylated proteins in DG after ischemia-reperfusion.

**Heat shock 70 kDa protein 1 (Hsp70.1).** Figure 5 shows the time course of specific oxidation levels of Hsp70.1 in the CA1 and DG. Our previous study demonstrated that Hsp70.1 was remarkably oxidized in the CA1 at days 3 and 5 after ischemia. On the

contrary, in the postischemic DG, carbonyl modification level of Hsp70.1 was increased only negligibly. Heat shock proteins (Hsps), being induced by stressful stimuli, are thought to support cellular integrity and viability. Hsp70.1 is a major protein of human Hsp70 family, and mainly functions as a chaperone enabling the cell to cope with harmful aggregations of denatured/damaged proteins during and after insults such as heat and ischemia.<sup>(26,27)</sup> In addition, the expression of Hsp70.1 at the lysosomal membrane confers its stability against cell stresses.<sup>(28–33)</sup> Previously, Sahara and Yamashita<sup>(34)</sup> demonstrated that carbonylated Hsp70.1 in the CA1 after ischemia was cleaved by activated  $\mu$ -calpain. Consequently, cleavage of Hsp70.1 leads to the membrane rupture with the resultant release of lysosomal protease cathepsins into the cytosol, which induced necrotic neuronal death in the CA1.<sup>(33,35)</sup> Our results demonstrated the specific oxidation level of Hsp70.1 was extensively increased in the CA1 after ischemia, although it was increased only negligibly in the DG. Carbonyl modification of Hsp70.1 in the CA1 may lead to loss

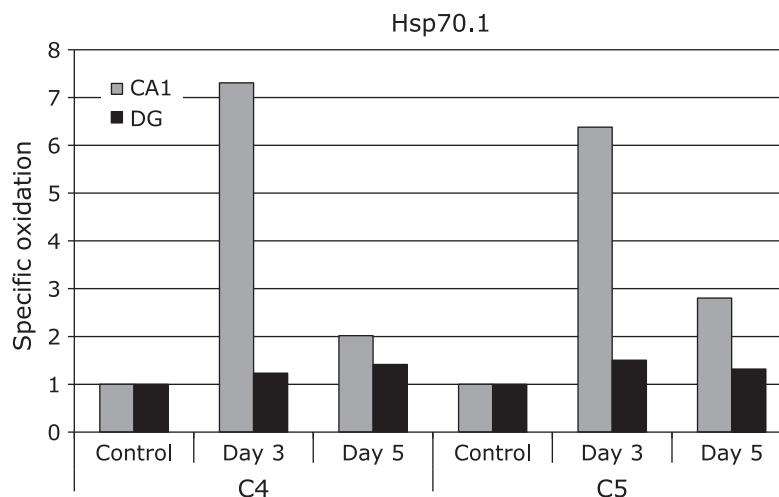


**Fig. 5.** The time course of specific oxidation level of Hsp70.1 in DG and CA1 after the ischemia-reperfusion. Spot numbers of DG region were used in 2D Oxyblot analysis using DG. Data of DG were compared with our previously reported data of CA1.<sup>(21)</sup>

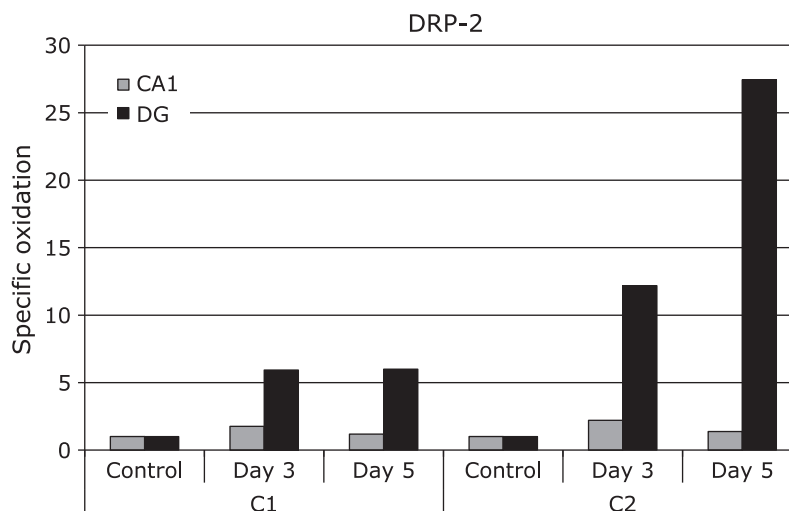


**Fig. 6.** The time course of specific oxidation level of DRP-2 in DG and CA1 after the ischemia-reperfusion. Spot numbers of DG region were used in 2D Oxyblot analysis using DG. Data of DG were compared with our previously reported data of CA1.<sup>(21)</sup>

of the neuroprotection, whereas intact Hsp70.1 may play an important role for the protection of DG against oxidative stresses after ischemia.

**Dihydropyrimidinase related protein 2 (DRP-2).** The specific oxidation levels of spot C1 and C2 were increased 5.99- and 27.43-fold, respectively, in the DG at day 5 after ischemia (Fig. 2). Both spots were identified as dihydropyrimidinase related protein 2 (DRP-2). DRP-2, also called ‘collapsing response mediator protein 2’ (CRMP-2) or ‘turned on after division-64 kD’ (TOAD-64), is a member of the CRMP/TOAD/Ulip/DRP family of cytosolic phosphoproteins. This protein family is involved in neuronal differentiation and axonal guidance, and found to be up-regulated after the focal brain ischemia.<sup>(36)</sup> DRP-2 is found abundantly in the nervous system, especially during development, and have also been found in adult brain.

Our previous results showed that the specific oxidation level of DRP-2 in the monkey substantia nigra at day 5 after ischemia was increased more than 4-fold.<sup>(37)</sup> Similarly, the specific oxidation level of DRP-2 in CA1 increased 2-fold on day 3 and 5 after

ischemia. Furthermore, our results showed that the specific oxidation levels of spots C1 and C2 of DRP-2 in the DG at day 5 after ischemia increased more than 5-fold and 20-fold, compared to that of carbonylated DRP-2 in CA1, respectively (Fig. 6). It is considered that multifunctional protein DRP-2 is one of major determinants in the control of oxidative stress.<sup>(38)</sup> Thus, a remarkably increase of specific oxidation level of DRP-2 in the postischemic DG may conceivably contribute to modulation of ischemic neuronal death. Fukui *et al.*<sup>(39,40)</sup> reported that ROS-derived phospho-DRP-2 expression may be associated with the induction axonal degeneration. Therefore, investigation is needed to clarify the expression level of phospho-DRP-2 induced by the oxidative damage due to ischemia reperfusion.

**L-Lactate dehydrogenase B chain (LDHB).** The specific oxidation level of spot C3 showed 17.7-fold increase in the DG at day 5 after ischemia (Fig. 2). Spot C3 was identified as L-lactate dehydrogenase B chain (LDHB). LDHB is terminal enzyme of anaerobic glycolysis, catalyze conversion of lactate into pyruvate.<sup>(41)</sup> L-lactate dehydrogenase (LDH) is a tetrameric enzyme formed by

combinations of two subunit (LDHA and LDHB), that catalyzes the reversible NAD-dependent interconversion of pyruvate to lactate.<sup>(42)</sup> LDH activity in rat brains declined with the increasing age,<sup>(43)</sup> and LDH activity reduced in hippocampus of mild cognitive impairment, which was correlated protein dysfunction and enzyme activity impairment.<sup>(44)</sup> Poon *et al.*<sup>(45)</sup> reported that LDH activity depression is caused by oxidative modification of enzyme. In addition, it is reported that LDH is carbonylated in the brain of SAMP8 mouse.<sup>(45)</sup> These results suggested that carbonylated LDHB have some effect on the decline in learning ability and memory processes in hippocampus by oxidative stress.

**Comparison of protein expression between DG and CA1 after ischemia-reperfusion.** Spot 1230 in Fig. 3 was identified as nicotinamide adenine dinucleotide (NAD)-dependent protein deacetylase sirtuin-2 (SIRT2). SIRT2 is widely accepted to be involved in ageing, energy production, and lifespan extension. SIRT2 expression is much higher in the brain than other organs, particularly in the cortex, striatum, hippocampus, and spinal cord.<sup>(46)</sup> The present study first demonstrated that SIRT2 was significantly increased in the DG at days 3, 5 and 7 after ischemia, but was decreased in the CA1 (Fig. 4). It was recently reported that SIRT2 was upregulated in ischemic neurons *in vitro* and *in vivo*.<sup>(47)</sup> Since SIRT2 activates an antioxidant enzyme, manganese superoxide dismutase (MnSOD),<sup>(48)</sup> it can regulate the cellular response to oxidative stress by reducing ROS. As SIRT2 can also deacetylate forkhead box O1 (FOXO1), it may reveal the protective effects against oxidative stress.<sup>(49)</sup> It is probable that upregulation of SIRT2 may contribute to the cell survival of the DG in response to the oxidative stress during the ischemia-reperfusion. Although further studies are needed to address a causal relationship between SIRT2 and cell death, SIRT2 should be a critical mediator of an oxidative stress response.

Other proteins such as inorganic pyrophosphatase and heat shock protein  $\beta$ -1 were significantly increased in the DG, but no significant changes were observed in the CA1. On the other hand, tropomyosin  $\alpha$ -3 chain, heat shock cognate 71 kDa protein, vesicle-fusing ATPase, enoyl-CoA delta isomerase 1 (mitochondrial) and PITH domain-containing protein 1 were significantly decreased in the postischemic DG. These proteins also did not show a significant change in the CA1.

Inorganic pyrophosphatase catalyzes conversion of one molecule of pyrophosphate to two phosphate ions. It was reported that inorganic pyrophosphatase partially protected the cells from apoptosis.<sup>(50)</sup> Cytosolic levels of inorganic pyrophosphatase have been shown to be increased in several proteomics studies dealing with cancer tissues such as lung and colon.<sup>(51,52)</sup> Heat shock protein  $\beta$ -1 (also known as HSP-27) is a member of a small heat shock protein family and is involved in the regulation of apoptosis, protection of cells against oxidative stress.<sup>(53)</sup> Interestingly, it is reported that heat shock protein  $\beta$ -1 is able to prevent  $\alpha$ -synuclein aggregation in the culture of neurons overexpressing  $\alpha$ -synuclein and thus increases neuron survival.<sup>(54)</sup> Thus, the increase in expression levels of inorganic pyrophosphatase and heat shock protein  $\beta$ -1 may play a neuroprotective role in the DG after ischemia.

Tropomyosins are family of microfilament-associated structural proteins. It was reported that tropomyosin  $\alpha$ -3 and -4 chain proteins participating in the cell motility were down-regulated in the vitamin C-induced apoptosis of human adenocarcinoma

AGS cells.<sup>(55)</sup> Tropomyosin stabilizes cytoskeleton actin filaments and as a result may participate in the morphological changes underlying hippocampal information processing.<sup>(56)</sup> Heat shock cognate 71 kDa protein serves to protect neurons by recycling aggregated proteins and reducing their toxicity.<sup>(57)</sup> Thus, down-regulation of tropomyosin  $\alpha$ -3 chain and heat shock cognate 71 kDa protein may be involved in the inhibition of apoptosis and neuroprotective in the DG after ischemia. Although enoyl-CoA delta isomerase 1 are involved in the basic mitochondrial function, the role of this protein is still unclear in the mechanism of cell survival in the DG after ischemia.

In conclusion, the DG is known to be extremely resistance to oxidative stress than the CA1 in hippocampus. In this study, the specific oxidation level of Hsp70.1 was extensively increased in the CA1 after ischemia, although it was not increased in the DG. In addition, the proteome analysis showed that the carbonyl levels of DRP-2 and LDHB were remarkably increased in the postischemic DG. Furthermore, protein expression level of SIRT2 was increased in DG, but it was decreased in CA1. We speculate that these proteins have the potential to be involved in the mechanism of resistance to oxidative stress in DG.

## Author Contributions

Contributors: Conceived and designed the study: SO and TY. Analyzed the data: SK, YK, YM, and ST-O. Wrote the paper: YM and SO. Paper modification: TY, HK and MM.

Ethics approval: The study was approved by the Animal Care and Ethics Committee of Kanazawa University (Approval No.: AP-132874).

## Acknowledgments

This work was supported by JSPS KAKENHI Grant Number 26293148, 15K15237, 18K19673 and 19H03885.

## Abbreviations

|            |   |
|------------|---|
| CA1        | cornu <i>Ammonis</i> 1  |
| 2D DIGE    | two-dimensional difference gel electrophoresis                                  |
| 2D Oxyblot | 2DE with immunochemical detection of protein carbonyls                          |
| 2DE        | two-dimensional gel electrophoresis   |
| DG         | dentate gyrus   |
| DNP        | 2,4-dinitrophenylhydrazine  |
| DNPH       | 2,4-dinitrophenylhydrazine  |
| DRP-2      | dihydropyrimidinase related protein 2   |
| FOXO1      | forkhead box O1   |
| Hsp70.1    | heat shock 70 kDa protein 1   |
| PMF        | peptide mass fingerprinting   |
| ROS        | reactive oxygen species   |
| SIRT2      | nicotinamide adenine dinucleotide (NAD)-dependent protein deacetylase sirtuin-2 |

## Conflict of Interest

No potential conflicts of interest were disclosed.

## References

- Cave AC, Brewer AC, Narayanapanicker A, *et al.* NADPH oxidases in cardiovascular health and disease. *Antioxid Redox Signal* 2006; **8**: 691–728.
- Sasaki M, Joh T. Oxidative stress and ischemia-reperfusion injury in gastrointestinal tract and antioxidant, protective agents. *J Clin Biochem Nutr* 2007; **40**: 1–12.
- Yenari MA, Giffard RG, Sapolsky RM, Steinberg GK. The neuroprotective potential of heat shock protein 70 (HSP70). *Mol Med Today* 1999; **5**: 525–531.
- Anwarullah, Aslam M, Badshah M, *et al.* Further evidence for the association of CYP2D6\*4 gene polymorphism with Parkinson's disease: a case control study. *Genes Environ* 2017; **39**: 18.
- Halliwell B. Reactive oxygen species and the central nervous system. *J Neurochem* 1992; **59**: 1609–1623.
- Coyle JT, Puttfarcken P. Oxidative stress, glutamate, and neurodegenerative disorders. *Science* 1993; **262**: 689–695.



- 7 Nakabeppu Y, Tsuchimoto D, Ichinoe A, *et al.* Biological significance of the defense mechanisms against oxidative damage in nucleic acids caused by reactive oxygen species: from mitochondria to nuclei. *Ann N Y Acad Sci* 2004; **1011**: 101–111.
- 8 Andersen JK. Oxidative stress in neurodegeneration: cause or consequence? *Nat Med* 2004; **10 Suppl**: S18–S25.
- 9 Avery SV. Molecular targets of oxidative stress. *Biochem J* 2011; **434**: 201–210.
- 10 Stadtman ER, Berlett BS. Reactive oxygen-mediated protein oxidation in aging and disease. *Chem Res Toxicol* 1997; **10**: 485–494.
- 11 Maisonneuve E, Ducret A, Khoueiry P, *et al.* Rules governing selective protein carbonylation. *PLoS One* 2009; **4**: e7269.
- 12 Levine RL. Carbonyl modified proteins in cellular regulation, aging, and disease. *Free Radic Biol Med* 2002; **32**: 790–796.
- 13 Benzi G, Moretti A. Are reactive oxygen species involved in Alzheimer's disease? *Neurobiol Aging* 1995; **16**: 661–674.
- 14 Bowling AC, Beal MF. Bioenergetic and oxidative stress in neurodegenerative diseases. *Life Sci* 1995; **56**: 1151–1171.
- 15 Brown RH Jr. Superoxide dismutase in familial amyotrophic lateral sclerosis: models for gain of function. *Curr Opin Neurobiol* 1995; **5**: 841–846.
- 16 Di Loreto S, Zimmiti V, Sebastiani P, Cervelli C, Falone S, Amicarelli F. Methylglyoxal causes strong weakening of detoxifying capacity and apoptotic cell death in rat hippocampal neurons. *Int J Biochem Cell Biol* 2008; **40**: 245–257.
- 17 Jesberger JA, Richardson JS. Oxygen free radicals and brain dysfunction. *Int J Neurosci* 1991; **57**: 1–17.
- 18 Love S. Oxidative stress in brain ischemia. *Brain Pathol* 1999; **9**: 119–131.
- 19 Serrano F, Klann E. Reactive oxygen species and synaptic plasticity in the aging hippocampus. *Ageing Res Rev* 2004; **3**: 431–443.
- 20 Pulsinelli WA, Brierley JB, Plum F. Temporal profile of neuronal damage in a model of transient forebrain ischemia. *Ann Neurol* 1982; **11**: 491–498.
- 21 Oikawa S, Yamada T, Minohata T, *et al.* Proteomic identification of carbonylated proteins in the monkey hippocampus after ischemia-reperfusion. *Free Radic Biol Med* 2009; **46**: 1472–1477.
- 22 Yamashima T, Saido TC, Takita M, *et al.* Transient brain ischaemia provokes Ca<sup>2+</sup>, PIP<sub>2</sub> and calpain responses prior to delayed neuronal death in monkeys. *Eur J Neurosci* 1996; **8**: 1932–1944.
- 23 Yamashima T, Kohda Y, Tsuchiya K, *et al.* Inhibition of ischaemic hippocampal neuronal death in primates with cathepsin B inhibitor CA-074: a novel strategy for neuroprotection based on 'calpain-cathepsin hypothesis'. *Eur J Neurosci* 1998; **10**: 1723–1733.
- 24 Bradford MM. A rapid and sensitive method for the quantitation of microgram quantities of protein utilizing the principle of protein-dye binding. *Anal Biochem* 1976; **72**: 248–254.
- 25 Kondo T, Hirohashi S. Application of highly sensitive fluorescent dyes (CyDye DIGE Fluor saturation dyes) to laser microdissection and two-dimensional difference gel electrophoresis (2D-DIGE) for cancer proteomics. *Nat Protoc* 2006; **1**: 2940–2956.
- 26 Hartl FU. Molecular chaperones in cellular protein folding. *Nature* 1996; **381**: 571–579.
- 27 Jäättelä M. Heat shock proteins as cellular lifeguards. *Ann Med* 1999; **31**: 261–271.
- 28 Bivik C, Rosdahl I, Ollinger K. Hsp70 protects against UVB induced apoptosis by preventing release of cathepsins and cytochrome c in human melanocytes. *Carcinogenesis* 2007; **28**: 537–544.
- 29 Doulias PT, Kotoglou P, Tenopoulou M, *et al.* Involvement of heat shock protein-70 in the mechanism of hydrogen peroxide-induced DNA damage: the role of lysosomes and iron. *Free Radic Biol Med* 2007; **42**: 567–577.
- 30 Gyrd-Hansen M, Nylandsted J, Jäättelä M. Heat shock protein 70 promotes cancer cell viability by safeguarding lysosomal integrity. *Cell Cycle* 2004; **3**: 1484–1485.
- 31 Mambula SS, Calderwood SK. Heat shock protein 70 is secreted from tumor cells by a nonclassical pathway involving lysosomal endosomes. *J Immunol* 2006; **177**: 7849–7857.
- 32 Nylandsted J, Rohde M, Brand K, Bastholm L, Elling F, Jäättelä M. Selective depletion of heat shock protein 70 (Hsp70) activates a tumor-specific death program that is independent of caspases and bypasses Bcl-2. *Proc Natl Acad Sci U S A* 2000; **97**: 7871–7876.
- 33 Nylandsted J, Gyrd-Hansen M, Danielewicz A, *et al.* Heat shock protein 70 promotes cell survival by inhibiting lysosomal membrane permeabilization. *J Exp Med* 2004; **200**: 425–435.
- 34 Sahara S, Yamashima T. Calpain-mediated Hsp70.1 cleavage in hippocampal CA1 neuronal death. *Biochem Biophys Res Commun* 2010; **393**: 806–811.
- 35 Yamashima T. Hsp70.1 and related lysosomal factors for necrotic neuronal death. *J Neurochem* 2012; **120**: 477–494.
- 36 Chen A, Liao WP, Lu Q, Wong WS, Wong PT. Upregulation of dihydropyrimidinase-related protein 2, spectrin alpha II chain, heat shock cognate protein 70 pseudogene 1 and tropomodulin 2 after focal cerebral ischemia in rats—a proteomics approach. *Neurochem Int* 2007; **50**: 1078–1086.
- 37 Oikawa S, Kobayashi H, Kitamura Y, *et al.* Proteomic analysis of carbonylated proteins in the monkey substantia nigra after ischemia-reperfusion. *Free Radic Res* 2014; **48**: 694–705.
- 38 Drabik A, Bierzynska-Krzysik A, Bodzon-Kulakowska A, Suder P, Kotlinska J, Silberring J. Proteomics in neurosciences. *Mass Spectrom Rev* 2007; **26**: 432–450.
- 39 Fukui K, Takatsu H, Koike T, Urano S. Hydrogen peroxide induces neurite degeneration: prevention by tocotrienols. *Free Radic Res* 2011; **45**: 681–691.
- 40 Fukui K, Masuda A, Hosono A, *et al.* Changes in microtubule-related proteins and autophagy in long-term vitamin E-deficient mice. *Free Radic Res* 2014; **48**: 649–658.
- 41 Ahn H, Lee K, Kim JM, *et al.* Accelerated lactate dehydrogenase activity potentiates osteoclastogenesis via NFATc1 signaling. *PLoS ONE* 2016; **11**: e0153886.
- 42 Baumgart E, Fahimi HD, Stich A, Völkl A. L-lactate dehydrogenase A4- and A3B isoforms are bona fide peroxisomal enzymes in rat liver. Evidence for involvement in intraperoxisomal NADH reoxidation. *J Biol Chem* 1996; **271**: 3846–3855.
- 43 Agrawal A, Shukla R, Tripathi LM, Pandey VC, Srimal RC. Permeability function related to cerebral microvessel enzymes during ageing in rats. *Int J Dev Neurosci* 1996; **14**: 87–91.
- 44 Reed T, Perluigi M, Sultana R, *et al.* Redox proteomic identification of 4-hydroxy-2-nonenal-modified brain proteins in amnesic mild cognitive impairment: insight into the role of lipid peroxidation in the progression and pathogenesis of Alzheimer's disease. *Neurobiol Dis* 2008; **30**: 107–120.
- 45 Poon HF, Castegna A, Farr SA, *et al.* Quantitative proteomics analysis of specific protein expression and oxidative modification in aged senescence-accelerated-prone 8 mice brain. *Neuroscience* 2004; **126**: 915–926.
- 46 Maxwell MM, Tomkinson EM, Nobles J, *et al.* The Sirtuin 2 microtubule deacetylase is an abundant neuronal protein that accumulates in the aging CNS. *Hum Mol Genet* 2011; **20**: 3986–3996.
- 47 Xie XQ, Zhang P, Tian B, Chen XQ. Downregulation of NAD-dependent deacetylase SIRT2 protects mouse brain against ischemic stroke. *Mol Neurobiol* 2016; **54**: 7251–7261.
- 48 Wang F, Nguyen M, Qin FX, Tong Q. SIRT2 deacetylates FOXO3a in response to oxidative stress and caloric restriction. *Ageing Cell* 2007; **6**: 505–514.
- 49 Zhao Y, Yang J, Liao W, *et al.* Cytosolic FoxO1 is essential for the induction of autophagy and tumour suppressor activity. *Nat Cell Biol* 2010; **12**: 665–675.
- 50 Lin HY, Yin Y, Zhang JX, *et al.* Identification of direct forkhead box O1 targets involved in palmitate-induced apoptosis in clonal insulin-secreting cells using chromatin immunoprecipitation coupled to DNA selection and ligation. *Diabetologia* 2012; **55**: 2703–2712.
- 51 Chen G, Gharib TG, Huang CC, *et al.* Proteomic analysis of lung adenocarcinoma: identification of a highly expressed set of proteins in tumors. *Clin Cancer Res* 2002; **8**: 2298–2305.
- 52 Tomonaga T, Matsushita K, Yamaguchi S, *et al.* Identification of altered protein expression and post-translational modifications in primary colorectal cancer by using agarose two-dimensional gel electrophoresis. *Clin Cancer Res* 2004; **10**: 2007–2014.
- 53 Felemban SG, Garner AC, Smida FA, Boock DJ, Hargreaves AJ, Dickenson JM. Phenyl saligenin phosphate induced caspase-3 and c-Jun N-terminal kinase activation in cardiomyocyte-like cells. *Chem Res Toxicol* 2015; **28**: 2179–2191.
- 54 Mymrikov EV, Seit-Nebi AS, Gusev NB. Large potentials of small heat shock proteins. *Physiol Rev* 2011; **91**: 1123–1159.
- 55 Nagappan A, Park HS, Park KI, *et al.* Proteomic analysis of differentially expressed proteins in vitamin C-treated AGS cells. *BMC Biochem* 2013; **14**: 24.
- 56 Fountoulakis M, Tsangaris GT, Maris A, Lubec G. The rat brain hippocampus proteome. *J Chromatogr B Analyt Technol Biomed Life Sci* 2005; **819**: 115–129.
- 57 Khan AT, Dobson RJ, Sattlecker M, Kiddle SJ. Alzheimer's disease: are blood and brain markers related? A systematic review. *Ann Clin Transl Neurol* 2016; **3**: 455–462.

This is an open access article distributed under the terms of the Creative Commons Attribution License, which permits unrestricted use, distribution, and reproduction in any medium, provided the original work is properly cited.